TECHNICAL PAPER

CrossMark

Dynamic analyses and preliminary design of offshore triceratops in ultra-deep waters

Srinivasan Chandrasekaran[1] · R. Nagavinothini[1]

Abstract

More adaptable geometric form of offshore platforms, counting on the benefits of form-dominant design, is effective to encounter various environmental loads. Offshore triceratops is a new-generation offshore platform, whose conceptual design showed good degree-of-adaptability to ultra-deep-water conditions. Deck is partially isolated from the buoyant legs by ball joints by allowing transfer of partial displacements of buoyant legs to deck but restraining transfer of rotational responses. Prior to the suitability assessment of triceratops for ultra-deep waters, detailed dynamic analysis on the preliminary geometric form is necessary as a proof of validation for design applications. Current study discusses a detailed numeric analysis of triceratops at 2400 m water depth under regular and irregular waves; preliminary design of both buoyant legs and the deck is also presented. Buoyant Legs are designed as stiffened cylinders and the deck is designed as the integrated truss system. In compliant structures, the role of tethers is of paramount importance. Hence, the stress analysis and fatigue analysis of the tethers are also carried out to assess the service life of the structure. Presented study shall aid offshore engineers and contractors to understand suitability of triceratops, in terms of design and dynamic response behaviour.

Keywords Triceratops · Offshore structures · Structural design · Ultra-deep water

Introduction

Oil and gas exploration is heading towards ultra-deep-water depth where even compliant platforms are not adaptable; large deck displacements impose limitations to their operational loads. More adaptable geometric form of offshore platforms, counting on form-dominant design is effective to encounter the loads. In deep waters, compliant structures are found to be cost effective [1–3]. Pre-tensioned Buoyant Leg platforms are said to have excellent motion characteristics and can be cost effective for marginal filed at ultra-deep waters [4–6]. Offshore triceratops is a new-generation offshore platform, whose conceptual design has good adaptability to ultra-deep-water conditions [7–9]. However, details of preliminary analyses and design at member level are s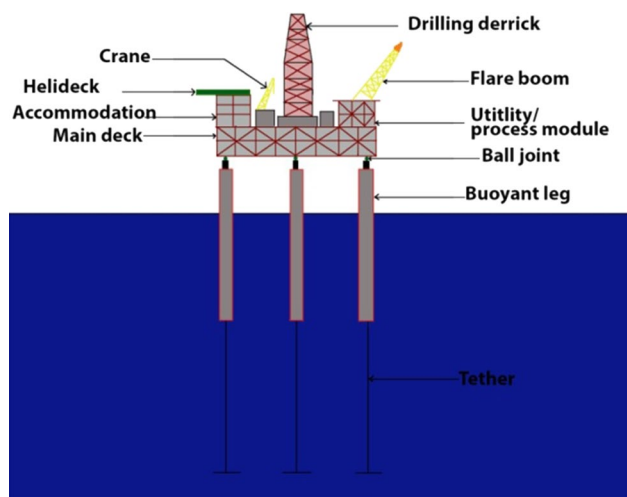carce in the literature. The preliminary analysis becomes important, as some design parameters may have significant effects on the structural behaviour in deep-water conditions [10]. Presented study shall aid offshore engineers and contractors to understand suitability of triceratops, in terms of design and dynamic response behaviour. Figure 1 shows the conceptual model of triceratops. Deck is partially isolated from the buoyant legs by ball joints. Displacements of buoyant legs under the encountered waves are transferred to the deck, but transfer of rotational response is restrained. While it enables to maintain the desired stiffness in vertical plane by monolithic action between the buoyant legs and deck, compliancy is not compromised in the horizontal plane. By restraining transfer of rotation to the deck, comfortable working environment to the people on board is ensured.

Deck is connected to three groups of buoyant legs; each group is position-restrained by a set of taut-moored tethers, which are commissioned under high initial pretension. Buoyant legs are deep-draft structures, which are similar to that of a Spar buoy. In addition, excess buoyancy and position-restraint characteristics are similar to a tension leg platform (TLP). Excess buoyancy ensures high initial pre-tension of tethers [11]. Buoyant legs are designed as stiffened cylindrical shell structures, as

✉ Srinivasan Chandrasekaran
drsekaran@iitm.ac.in

R. Nagavinothini
vino.civil35@gmail.com

[1] Department of Ocean Engineering, Indian Institute of Technology Madras, Chennai, India

Fig. 1 Conceptual model of triceratops

Table 1 Details of triceratops

Description	Unit	Quantity
Water depth	m	2400
Density of steel	kg/m³	7850
Density of sea water	kg/m³	1025
Geometric details		
Diameter of leg	m	15
c/c distance between the legs	m	61.77
Length of the leg	m	174.24
Freeboard	m	20.24
Draft	m	154
Tether length	m	2246
Diameter of tether	m	1.00
Vertical centre of gravity of BLS	m	− 112.74
Meta-centric height	m	35.83
Load details		
Self-weight + payload	kN	562,424
Buoyancy force	kN	820,932
Total tether force	kN	258,491
Structural properties		
Area of deck	m²	3933
Area of tether	m²	2.356
Stiffness of tethers	GN/m	0.22

they are found to be suitable for application in offshore structures [12]. Similar to that of TLPs, increase in cost of triceratops is only due to the mooring system and its installation in deep waters, not due to the geometric form. Experimental and numerical investigations carried out by previous researchers discussed the operational advantages of the structural configuration, reduced deck response, and good re-centering capability [7]. Experimental and analytical studies showed that the coupled responses of the deck in rotational degrees-of-freedom are lesser than that of the buoyant legs [13]. The presence of ball joints is advantageous even under the seismic action of triceratops [14]. Stiffened triceratops are the modified geometric forms, whose response behaviour showed improvement even under impact loads [7]; under impact loads, bursts are seen in heave response, but with no rapid built-ups. Beat phenomenon occurs in all degrees-of-freedom, but with a lower magnitude in sway and roll [15].

Prior to the suitability assessment of triceratops for ultra-deep waters, detailed dynamic analysis on the preliminary geometric form is necessary as a proof of validation for design applications. Current study discusses a detailed numeric analysis of triceratops at 2400 m water depth; preliminary design of both buoyant legs and the deck are also presented. Natural periods in different degrees-of-freedom are determined, followed by detailed dynamic analysis under both regular and irregular waves; stress analysis of tethers is also carried out for estimating possible fatigue failure. This study is a preliminary investigation for assessing suitability of triceratops for ultra-deep water. The coupling effect due to wind and waves on the platform is ignored. The study involves the modelling and analysis of the buoyant legs and deck only; effects of risers are not considered in the analysis.

Preliminary design of buoyant legs

Geometric form of triceratops is developed on the basis of dimensions of PERDIDO Spar [16]. Triceratops is modelled with the same height as that of the hull of Spar, while buoyancy of the hull form is equally distributed to three buoyant legs. Topside weight is maintained as same as that of the Spar platform with three-tier deck, similar to that of a typical drilling platform. Geometric details and structural properties are given in Table 1. Triangular-shaped deck is chosen for the symmetric distribution of lateral load amongst the buoyant legs.

Buoyant legs are preferably designed as stiffened cylinders as they are required to resist both axial stress and bending moment caused by lateral forces. Stiffeners are integrally welded to the shell to enhance their lateral resistance. In addition, longitudinal stiffeners (called as stringers) are also provided at equal spacing, both externally and internally. Such orthogonally stiffened cylinder can fail by shell buckling, panel stiffener buckling, panel ring buckling, general buckling, and column buckling [11]. Comparing similar structural configurations subjected to such complex failure modes, preliminary design parameters of the platform are fixed. Table 2 shows the summary of design parameters. Environmental conditions are chosen for Gulf of Mexico; corresponding values of sea state are mentioned in Table 2.

Table 2 Preliminary design parameters

Description	Value
Diameter of buoyant leg	15 m
Length of the buoyant leg	174.54 m
Thickness of shell	40 mm
Stringer system	Flat bar (70 numbers)
Ring frame system	Flat bars at 3 m apart
Restraining system	4 tethers per leg
Topside weight	97.4 MN
Payload	165 MN
Buoyant leg and tether weight	209 MN
Ballast weight	91.6 MN
Total displacement	562.4 MN
Environmental criteria	
Water depth	2400 m
Wave height	
100 years	23.7 m
1 year	7.9 m
Peak period	
100 years	14.0 s
1 year	9.1 s
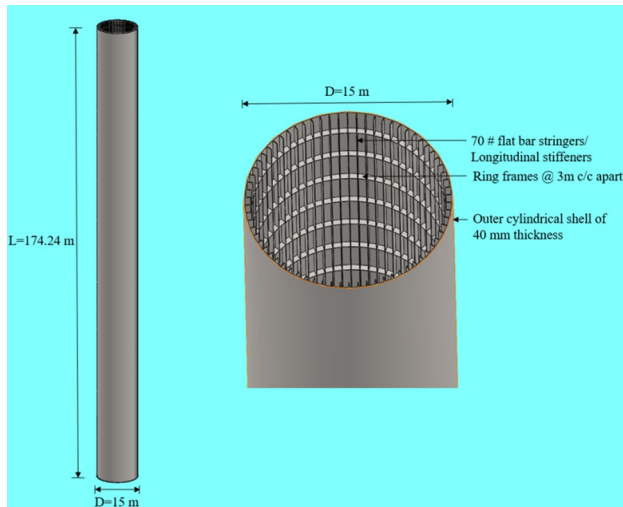
Fig. 2 Stiffened cylindrical shell and buoyant leg

Buoyant legs are sized as cylindrical shell of 15 m diameter and 174.24 m long, with rings and stringers, placed at equal spacing; shell thickness is varied from 15 to 40 mm. High strength steel is chosen for cylindrical shell, rings, and stringers. Cylindrical shell is provided with 70 stringers of 300×40 mm flats. While rings are spaced at 3 m c/c as orthogonal stiffeners, heavy ring frames are provided at the ends of the shell. Figure 2 shows the cylindrical shell and buoyant legs with stiffeners. Buckling strength and stability check are performed as per code provisions [17]. Stiffened

cylinder dimensions are checked against different buckling modes. Detailed finite-element analysis has to be performed to include geometric imperfections and residual stresses in the cylindrical structure. Buoyant leg should be fabricated in segments and welded together; lower compartment has to be ballasted after installation.

Shell buckling

Elastic buckling strength is given by

$$S_E = A \frac{\Pi^2 E}{12(1 - v^2)} \left(\frac{t_s}{s_s} \right), \qquad (1)$$

where A is reduced buckling coefficient, which depends upon the stress condition, E is Modulus of elasticity of steel, v is Poisson's ratio (0.3), t_s is shell thickness, and s_s is spacing between longitudinal stiffeners. The characteristic buckling stress of shell is found to be 557 N/mm^2, which is greater than the yield stress.

Panel ring buckling

Panel buckling is avoided by proportioning the ring stiffeners properly. Design should satisfy the required cross-sectional area and moment of inertia, including the effective width of the shell plate. Buckling strength is then computed for the flat bar ring frame, by considering the effective supports of stiffened cylinder. In the present study, stiffened cylinder is assumed to have heavy ring frames at the ends. The buckling stress of longitudinally stiffened cylinder is 600 N/mm^2.

Column buckling

It is computed using the following relationship:

$$S_C = \left[1 - 0.28\alpha^2 \right] S_a \quad \text{for} \quad \alpha \le 1.34, \qquad (2)$$

$$S_C = \frac{0.9}{\alpha^2} S_a \quad \text{for} \quad \alpha > 1.34, \qquad (3)$$

where α is reduced column slenderness, and S_a is reduced characteristic buckling strength. The column buckling stability criterion is satisfied as the design equivalent Von Mises Stress (457 N/mm^2) is found to be less than the characteristic buckling stress. Hence, the design criterion is satisfied.

Preliminary design of deck

Drilling, production, and residential space are sufficiently provided on the deck to cater all operational requirements. A modular unit of topside weighing about 20,000–40,000 t supported on a heavy tubular framed structure is chosen for

the top side. Modular frame support is a heavy tubular structure, which can be alternated by integrated decks, resulting in a lighter deck. However, in both the cases, method of design is almost similar [18]. Weight of the drilling derrick, deck supplies, production equipment, and other topside components is applied as direct load on the deck, which is transferred to the buoyant legs. Topside is designed with three deck levels: cellar deck, main deck, and top deck. The deck is designed as the integrated truss deck system with the floor made up of truss-type connection for the main deck flooring and beam panel arrangement on the cellar deck and top deck flooring. Truss-type deck supports the main deck of the topside while flooring of cellar deck and top deck (placed above cellar) is designed as beam-plate-type construction. Alternatively, floor may also be designed as corrugated steel or composite floor panel. Truss system is stiffened with diagonal members to resist wind loads. Dead load includes self-weight of the platform, weight of equipments and ballast material, hydrostatic pressure, and axial pre-tension force on tethers. Live load includes weight of personnel, non-permanent equipments, operational loads, and impact loads. Based on the conditions related to the normal use

and operation, live load varies in magnitude, direction, and position. Data provided by the equipment manufacturers are critically evaluated to compute the live loads; they are applied as point loads over an area of 0.3 m × 0.3 m. Each component of the deck is designed based on the bending moment considerations. Design considerations of the deck are summarized in Table 3.

Numerical analyses

Numerical analysis is carried out using ANSYS AQWA. This software can simulate the linearized hydrodynamic fluid wave loading, by three-dimensional radiation theory or diffraction theory. In time-domain dynamic simulation, real-time motion of a floating body is simulated at each time step by integrating accelerations in time domain using predictor–corrector integration scheme. Buoyant legs are modelled as line elements in ANSYS AQWA, as they are Morison elements ($D/L < 0.2$). Mass of buoyant legs and ballast loads are applied at the mass centre of each group of legs. The buoyant legs are defined as

Table 3 Design considerations of deck

Description	Value
Shape of the deck	Triangular deck
Length of the deck	95 m
Number of decks	3
Number of bays in the truss	9
Length of each bay	9.5 m
Load details	
Total topside weight	97.4 MN
Live load in process and drilling zone	5 kN/m^2
Live load in storage floors	18 kN/m^2
Sustained wind speed	55.88 m/s
Initial tether tension	28,721 kN
Design considerations	
Factor of safety for deal and live load	1.3
Type of steel	High strength steel
Size of deck components	
Thickness of deck plate	100 mm
Transverse beam	Wide flange beam W 27 × 114
Longitudinal beam	Back to back channel section stiffened with flange plates: Web = 700 × 30 mm Flange = 350 × 30 mm
Open web joist type	k-series
Depth of web joist	710 mm
Diameter of web joist members	20 mm
Main chord members of truss	Channels, back to back
Diagonal members of truss	Tubular members
Diameter and thickness of diagonal members	800; 12 mm
D/t ratio of truss diagonal members	40

TUBE elements and Morison equation is used for calculating the wave force:

$$q_n = \frac{1}{2}\rho C_d dA(v_n - \dot{x}_n)|v_n - \dot{x}_n| + \rho dV a_n + (C_m - 1)\rho dV(a_n - \ddot{x}_n),$$
(4)

where v_n and a_n are water particle velocity and acceleration, respectively; $\dot{x}_n$ and $\ddot{x}_n$ are velocity and acceleration of the structure; C_d is drag coefficient, C_m is the inertia coefficient, ρ is the density of sea water, and dA and dV are the exposed area and displaced volume per unit length, respectively. The drag and inertia coefficients are taken as 0.75 and 1.0, respectively. Three point Gaussian integration scheme is used for the calculation of hydrodynamic force. Weight of the deck and payload is applied at the mass centre of deck. Each group of buoyant legs is connected to the deck using ball joints. Tethers are modelled as cable elements with appropriate axial stiffness and stretched up to impart the desired initial tension. Tethers extend from the keel of the each buoyant leg group to the seafloor. Numerical model is shown in Fig. 3. Meshing of the developed model is done by three-dimensional panel method. Modelling is followed by assessing the critical hydrostatic parameters to assess its stability and operability in ultra-deep water. Table 4 summarizes the critical parameters of buoyant leg. By convolution integration technique, the following equation of motion is solved:
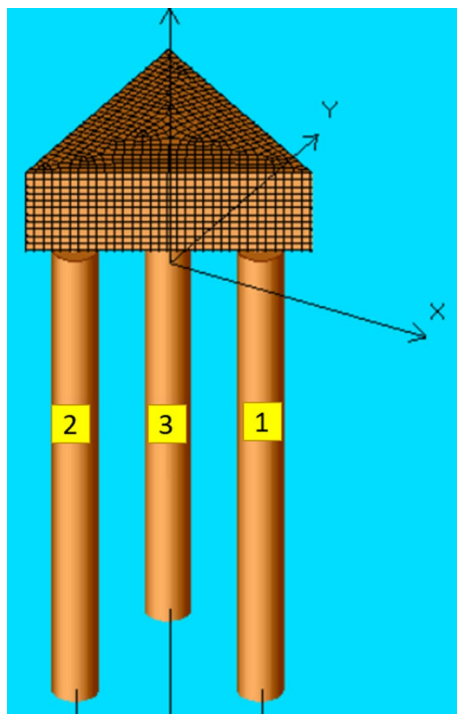
$$[M + M_a]\ddot{x}(t) + [C]\dot{x}(t) + [K]x(t) = F(t),$$
(5)

Fig. 3 Numerical model of triceratops

Table 4 Hydrostatic parameters of buoyant leg

Description	Value
Cut water plane properties	
Cut water plane area	176.7 m²
Principal second moment of inertia	2487 m⁴
Small angle stability parameters	
Distance between centre of gravity and centre of buoyancy	− 35.74 m
Distance between metacentre and centre of buoyancy (BM)	0.9131 m
Meta-centric height (GM)	35.83 m

where $\ddot{x}(t)$, $\dot{x}(t)$, $x(t)$, and $F(t)$ are acceleration, velocity, displacement, and force vectors, $[M]$ is the structural mass matrix, M_a is the added mass matrix, $[C]$ is the damping matrix, and $[K]$ is the stiffness matrix.

Free oscillation studies

Free oscillation studies are carried out to determine natural period and damping of the platform. One of the main advantages of the buoyant leg-supported structures is its free-floatation characteristics. Free oscillation test in different degrees-of-freedom is performed numerically by giving external disturbing forces in the respective degrees-of-freedom, to measure the free vibration responses. Damping is estimated based on the free oscillation test carried out on the numerical models, by logarithmic decrement method. Table 5 summarizes natural period and damping ratios in different degrees-of-freedom of free-floating buoyant leg units. It is seen from the table that natural periods of buoyant leg units, in roll and pitch, are found to be greater than dominant wave periods (5–20 s). This confirms the convenience of installation and commissioning of buoyant leg groups [19]. However, heave period of the free-floating buoyant leg lies in the wave period zone, which necessitates additional care during installation or decommissioning.

Free oscillation studies are subsequently carried out on tethered triceratops. Natural periods and damping ratio in various degrees-of-freedom are given in Table 6. The results are compared with the natural period and damping ratio of stiffened triceratops [13]. As observed from the table,

Table 5 Natural period and damping of free-floating buoyant leg

Description	Natural period (s)	Damping ratio (%)
Heave	19	0.24
Roll	151.9	1.14
Pitch	151.9	1.14

Table 6 Natural period and damping of tethered triceratops

Degree-of-freedom	Present study		Chandrasekaran and Madhuri [20]	
	Natural period (s)	Damping ratio (%)	Natural period (s)	Damping ratio (%)
Surge	215.0	5.84	88.4	8.15
Sway	215.4	5.87	88.4	8.15
Heave	4.3	0.94	1.8	1.08
Roll	6.2	6.11	9.46	4.34
Pitch	6.1	6.10	9.46	4.34
Yaw	215.9	6.23	–	–

high periods in surge, sway, and yaw degrees-of-freedom confirm high degree-of-compliancy in horizontal, while low periods in heave, roll, and pitch confirm stiff motion in vertical plane. High initial pre-tension restrains roll and pitch motion, in comparison with that of its free-floatation characteristics. Higher natural period of tethered triceratops is observed in the present study. Similarly, there is a discrepancy in the damping ratio in rotational and translational degrees-of-freedom. This may be attributed to the difference in the water depth, initial pre-tension, and the type of buoyant leg.

Dynamic response under regular waves

Numerical analysis is carried out in ANSYS AQWA for different sets of wave height and period of waves. Response history of the deck is plotted in active degrees-of-freedom under unidirectional regular waves. Figure 4 shows response of the deck under (6 m, 15 s) regular waves, very rough sea state under Douglas sea scale. It is seen from the figures that surge response is periodic, while

Fig. 4 Deck response under regular waves in very rough sea state

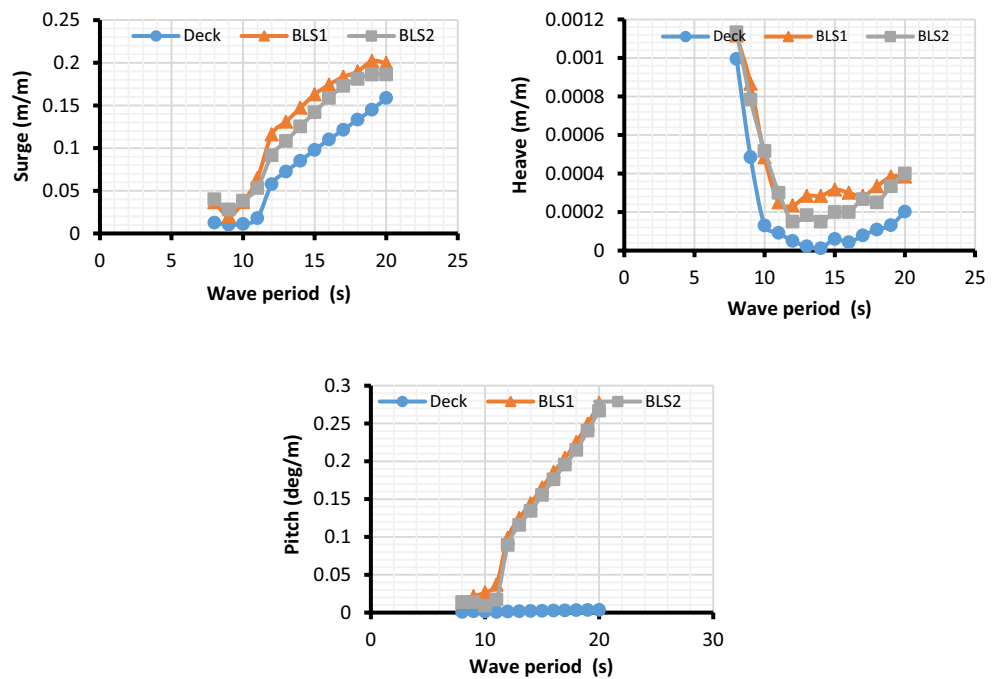**(a)** Surge
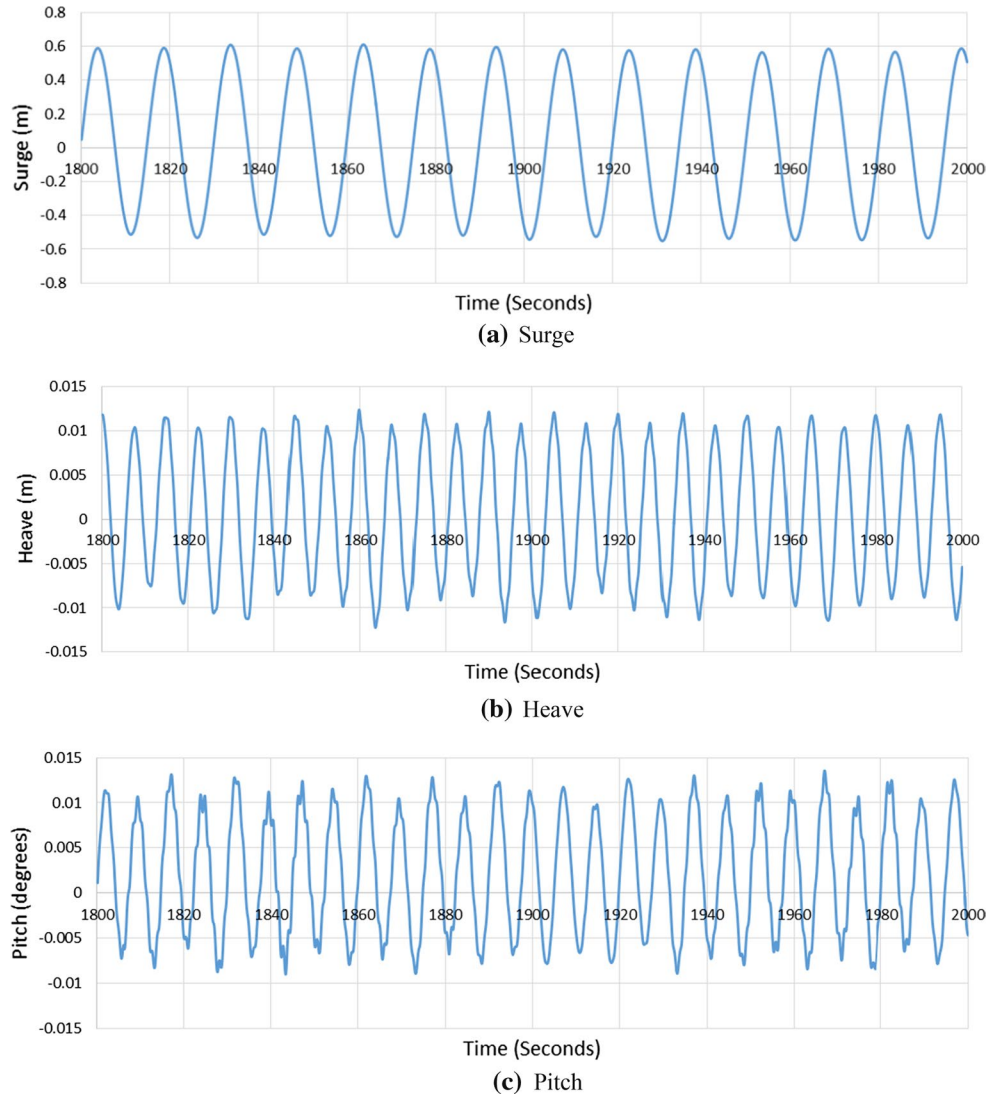
(b) Heave

(c) Pitch

heave and pitch response fluctuates around the mean position and is repeated throughout the time history. Response is examined under different wave heights of 2, 4, and 6 m under unidirectional waves. These sea states can be described as moderate, rough, and very rough under Douglas sea scale. Figure 5 shows Response Amplitude Operators (RAO) in active degrees-of-freedom in very rough sea state; response for other wave height and periods is given in Table 7. It is seen that deck response is lower than that of buoyant leg groups in translational degrees-of-freedom; pitch response of the deck is negligible. Triceratops show reduced responses for higher amplitude waves compared to that of lower amplitude waves. Figure 6 shows deck

response under different wave-heading angles for 6 m wave height.

Deck response in surge degree-of-freedom influences all operational activities in the drilling platform. Though surge responses are not easily excited, the response is mainly due to coupling between surge and pitch degrees-of-freedom, resulting from differential tension variation in tethers. Deck response at wave period of 15 s under 120° is lower than that of 0° and 180° by 54 and 50%, respectively. Heave motion is responsible for the dynamic tether tension variation. As seen from the figures, heave response attains maximum value at the pitch natural period and then reduces gradually. The presence of ball joints

Fig. 5 Response under regular waves in very rough sea state

Table 7 Deck response under zero wave-heading angle for different wave heights

Wave period (s)	Wave height = 2 m			Wave height = 4 m			Wave height = 6 m		
	Sea state: moderate			Sea state: rough			Sea state: very rough		
	Surge	Heave	Pitch	Surge	Heave	Pitch	Surge	Heave	Pitch
8	0.0376	0.00058	0.0036	0.0752	0.00116	0.0072	0.0756	0.0054	0.0048
9	0.078	0.00054	0.002	0.15612	0.00108	0.004	0.0612	0.0024	0.0102
10	0.1392	0.0005	0.0016	0.2784	0.001	0.0032	0.066	0.00078	0.0078
11	0.2012	0.0006	0.0018	0.4024	0.0012	0.0036	0.1074	0.00054	0.0036
12	0.2586	0.00036	0.0024	0.5172	0.00072	0.0048	0.3462	0.0003	0.0078
13	0.328	0.00028	0.0028	0.656	0.00056	0.0056	0.435	0.00012	0.0102
14	0.4162	0.00038	0.003	0.8324	0.00076	0.006	0.5106	0.00006	0.012
15	0.4916	0.00044	0.0034	0.9832	0.00088	0.0068	0.5874	0.00036	0.0132
16	0.5344	0.0004	0.0032	1.0688	0.0008	0.0064	0.6606	0.00024	0.015
17	0.5618	0.00062	0.0034	1.1236	0.00124	0.0068	0.7284	0.0048	0.0168
18	0.6096	0.0008	0.0038	1.2192	0.0016	0.0076	0.7998	0.0006	0.018

Fig. 6 Deck response under different wave-heading angles in very rough sea state
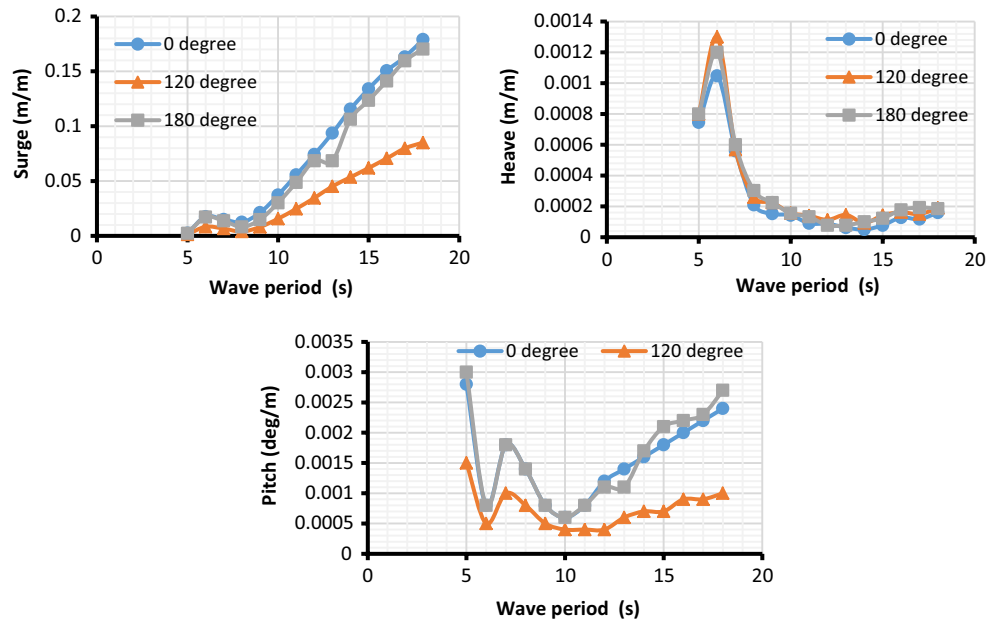
reduces the deck response than that of the buoyant legs, which shows operational advantage of triceratops in ultra-deep waters. Since the amplitude of motion is very small, this will prevent the flexural yielding of the drilling risers. At a wave period of 15 s, heave response of the deck is 60, 76, and 81% lower than that of the buoyant legs, which is quite significant. Heave response of the deck under 120° is about 24 and 8% higher than that of the response at 0° and 180°, respectively. Reduced pitch response of the deck is attributed to the presence of ball joints. However, pitch response seen in the deck arise from the differential heave response of the buoyant legs, as transfer of heave motion is not completely restrained by the ball joints. It is seen from the figures that pitch response starts increasing after reduction in heave response, which is due to the coupling effect between different degrees-of-freedom. Pitch response in the buoyant legs under different wave heights increases with the increase in time period.

Validation of results

The obtained response under regular waves in surge, heave, and pitch degrees-of-freedom are compared with the response of stiffened triceratops obtained from numerical studies by Chandrasekaran and Madhuri [20]. RAO at a wave period of 15 s are given in Table 8. The response in all degrees-of-freedom in the present study is lesser than that of the values reported in the literature. This shows the adequacy of triceratops in ultra-deep waters. However, the variation arises due to the change in the tether tension, water depth, and type of platform.

Table 8 Validation of results

Degrees-of-freedom	Present study	Chandrasekaran and Madhuri [20]
Surge (m/m)	0.0979	0.38
Heave (m/m)	0.00006	0.0025
Pitch (deg/m)	0.0022	0.03

Dynamic response under random waves

Assessment of response under random sea is necessary to determine the stress variation on members. Random sea state is defined by significant wave height (H_s) and zero crossing periods (T_z). Sea state is assumed to be zero-mean ergodic process and it is defined by the wave spectrum. Selection of the spectrum depends upon the frequency characteristics of the wave environment. Time-domain analysis is performed in the numerical model using the following wave spectra:

Pierson Moskowitz spectrum (PM)

It is a two-parameter spectrum suitable for open sea conditions, developed by relatively moderate winds over large fetches. It is given by the following relationship:

$$S^+(\omega) = \frac{1}{2\pi} \frac{H_s^2}{4\pi T_z^2} \left(\frac{2\pi}{\omega} \right)^2 \exp\left(-\frac{1}{\pi T_z^4} \left(\frac{2\pi}{\omega} \right)^4 \right), \qquad (6)$$

where H_s is significant wave height, T_z is zero crossing period, and ω is frequency.

JONSWAP spectrum

It is a modified form of PM spectrum and it is recommended in North Sea. This spectrum is used only for limited fetch to describe the winter storm waves. It is used to describe the wave system with imbalance in the energy flow and it is used very widely for the reliability analysis. It is given by the following relationship:

$$S^+(\omega) = \left(\frac{\bar{\alpha}g^2}{\omega^5}\right)e^{\left[-1.25\left(\frac{\omega}{\omega_o}\right)^{-4}\right]}\gamma^{a(w)} \tag{7a}$$

Fig. 7 Spectral plots used in the study (15 m, 15 s)

$$a(w) = e^{\left[-\frac{(\omega-\omega_o)^2}{2\bar{\sigma}^2\omega_o^2}\right]} \tag{7b}$$

$$\bar{\sigma} = \begin{cases} 0.07 & \text{for} \quad \omega \leq \omega_o \\ 0.09 & \text{for} \quad \omega > \omega_o \end{cases} \tag{7c}$$

$$\bar{\alpha} = \left(3.25 \times 10^{-3}\right)H_s^2\omega_o^4[1 - 0.287\ln(\gamma)] \tag{7d}$$

where $\bar{\sigma}$ is spectral width parameter, ω_o is significant frequency, $S^+(\omega)$ is spectral density, and γ is peakedness parameter (varies from 1 to 7). Spectral plots, used as the input for analysis, are shown in Fig. 7. As seen in the figure, maximum peak occurs at the frequency ratio (wave frequency/peak frequency) of unity. As both the spectra are plotted for 15 s wave period, peak frequency is occurring at 0.42 rad/s (= $2\pi/15$). Numerical analysis is carried out under both the spectra, for significant wave height of 15 m and wave period of 15 s. Response of the deck in all active degrees-of-freedom is shown in Figs. 8 and 9, for P–M spectrum and JONSWAP spectrum, respectively. The power spectral density plot shows the energy content of the response [21]. As seen from the response under PM spectrum, maximum amplitude occurs at the neighbourhood of peak wave frequency; amplitude is also significantly higher than that of the PSD of JONSWAP. Furthermore, heave and pitch responses under JONSWAP spectrum have maximum amplitude at the neighbourhood of 0.8 rad/s, while maximum surge response occurs at the vicinity of peak wave frequency.
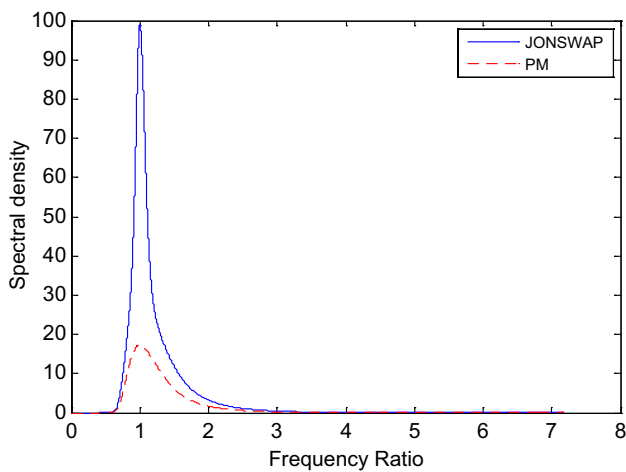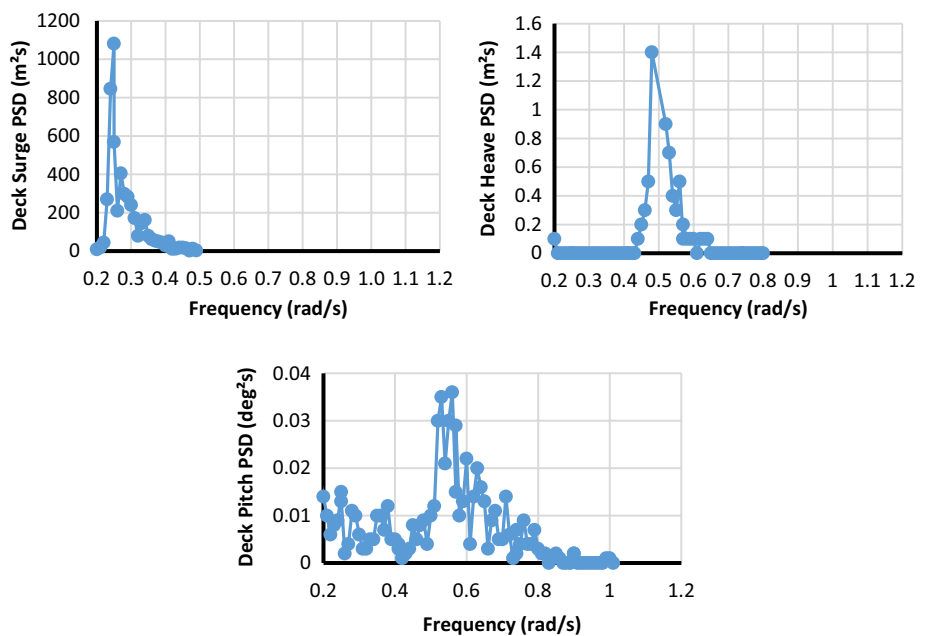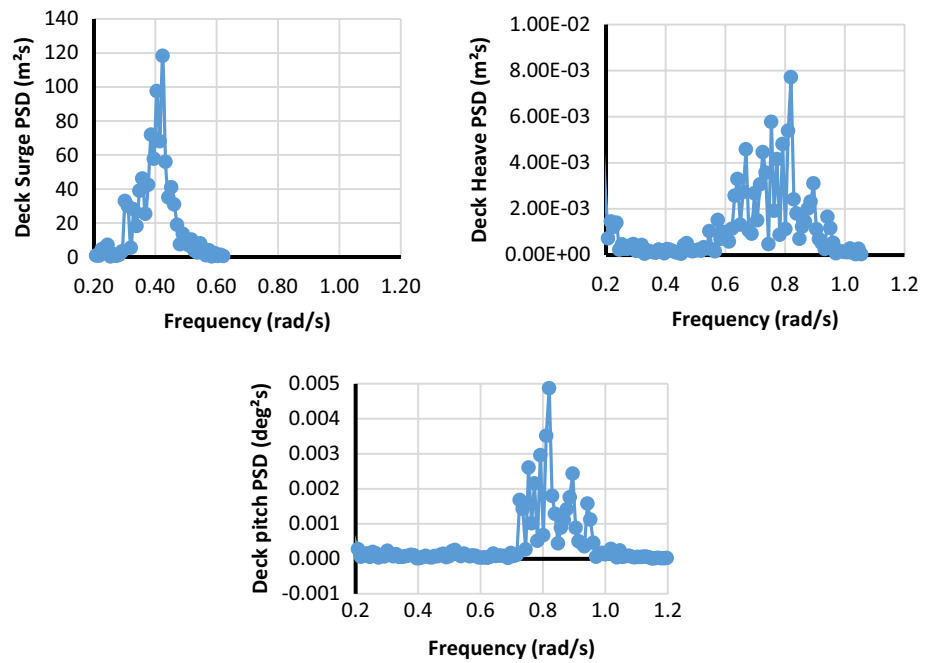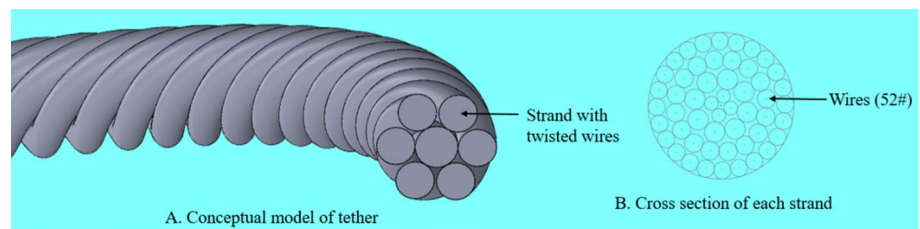

Fig. 8 Deck response under PM spectrum (15 m, 15 s)

Fig. 9 Deck response under JONSWAP spectrum (15 m, 15 s)

Fig. 10 Numeric model of tether

Stress analysis of tethers

Tethers are manufactured using wired ropes of stainless steel or carbon steel. Metallic wires are twisted around the central core to form a strand; the number of strands is twisted in a certain pattern to form a metallic wire ropes. The strength and ductility of each wire are accounted for use as tethers. Figure 10 shows mode of tether used in the study.

Each group of buoyant legs is position-restrained by a set of tethers, consisting of three numbers. They are 2246 m long, whose core diameter of 100 mm, consisting of high strength steel (7×52) with left lay-regular lay arrangement. 52 wires are laid around the central core in an opposite direction to strands, which are laid around the core. Wire ropes are protected against corrosion by providing polyurethane covering. Breaking stress of the steel wires is considered as 1500 N/mm². One of the main advantages of using wired strands is to achieve high strength-to-weight ratio, low elongation, reduced rotation characteristics, and high endurance limit. Table 9 shows the structural properties of tethers used in the present study.

Table 9 Properties of tethers

Item	Characteristics
Type of arrangement	Left lay-regular lay
Number of tethers	9
Length of the tethers	2246 m
Diameter of wire	100 mm
Number of wires	52
Number of strands	7
Area of tether	2.356 m²
Stiffness of tether	0.22 MN/m
Yield stress of wires	500 N/mm²
Breaking stress of wires	1500 N/mm²

Under wave loads, buoyant legs undergo large displacements and rotation about the ball joints. As each group of buoyant legs is not inter-connected, their motion is independently transferred to the deck. As a result, each group of tethers undergoes dynamic tether tension variation. This may result in Mathieu type of instability [13]. Figure 11 shows dynamic tether stress variation in buoyant
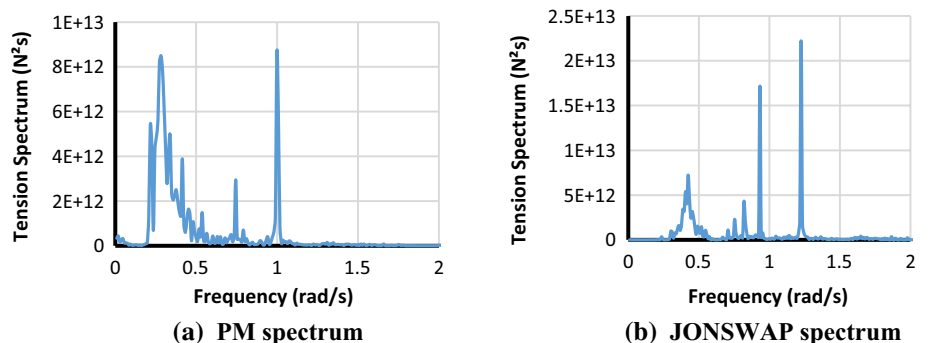
Fig. 11 Stress variation in tethers in rough sea state
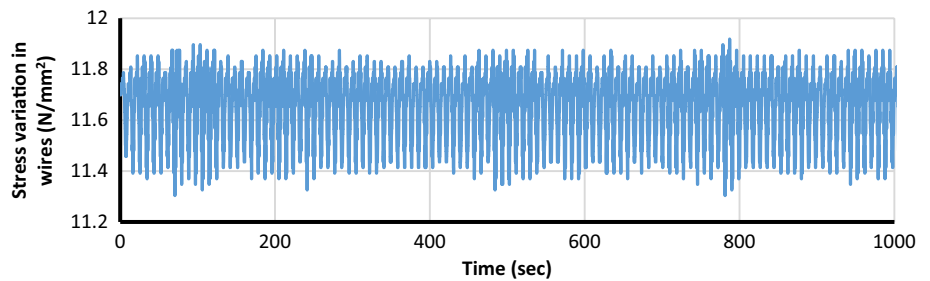
leg-1, under regular waves in rough sea state. Maximum and minimum tension variation is observed as 0.3 and 0.28 MN, which is about 1.7 and 3.6% of that of the initial pre-tension. Maximum stress developed in each wire is found to be 12 N/mm^2, which is much lower than the yield strength. Similarly, maximum tension variation observed in phenomenal sea state is observed as 19% of that of the initial pre-tension, which developed a maximum stress of about 28 N/mm^2, which is only 6% of that of its yield stress. It is evident that the chosen configuration of tether is adequate under both the sea states and shall not cause tether pullout. Tether tension variations are found out to be periodic in nature, which is predominantly governed by the behaviour of regular waves. Hence, low-amplitude, large cycle effects such as fatigue may become important.

Dynamic tension variation in tethers is also examined under random waves. Based on the numerical analysis carried out under random waves using PM spectrum and JONSWAP spectrum, power spectral density plots of tension variation in buoyant leg-1 are shown in Fig. 12. From the tension spectrum under PM spectrum, it is seen that the maximum tension occurs at a frequency of about 1.02 rad/s, which is closer to roll and pitch natural frequencies; instantly, a major peak is also seen in the neighbourhood of the peak wave frequency. On the other hand, tension spectrum under JONSWAP shows maximum amplitude at about 1.48 rad/s, which is closer to the heave natural frequency.

Service life estimation of tethers

The service life of the structure is estimated based on the service of the tethers for the compliant systems, as the pull out of any one of the tether may lead to failure of the structure. To find the service life of the structure, fatigue analysis is carried out. The tether tension variation under regular and irregular waves is presented. The stress time history is obtained from the tether tension variation, and then, using rain-flow counting method, the stress histogram is plotted. The histogram gives the stress range with the number of cycles. The allowable number of cycles is calculated as per DNV-RP-C203 [22]. The fatigue parameters where chosen for the material in sea water. The fatigue design is based on the S–N curves. The S–N relationship is given by
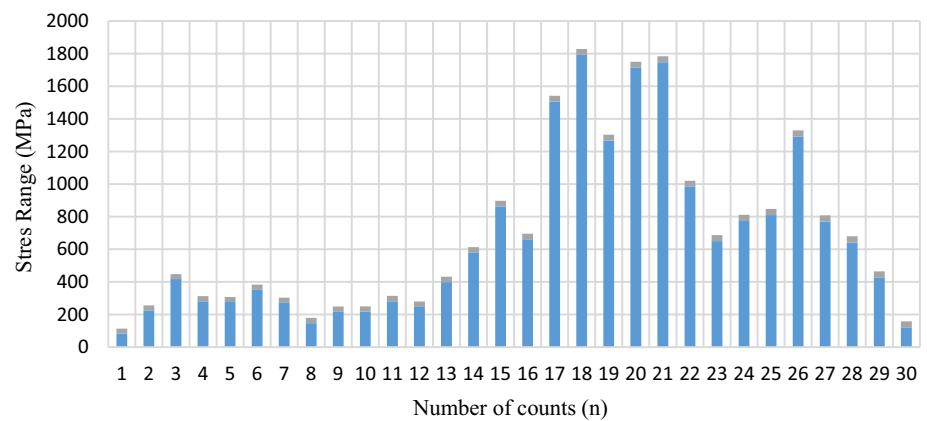
$$\log N = \log A - m \log S \tag{8}$$

where N is the number of allowable cycles, S is the stress range, and A and m are the constants obtained from the S–N curves. Then, the fatigue damage is calculated by Palmgren–Miner's Rule, which is given by

$$D = \sum_{i=1}^{m} \frac{n_i}{N_i} \tag{9}$$

where D is the fatigue damage, n is the number of counts from the histogram, and N is the number of allowable cycles from S–N relationship. The calculated fatigue life is extrapolated to get the service life. The service life of the structure under rough sea state is found out to be 20.03 years, whereas under phenomenal sea state (WH = 24 m, T = 14 s), it is

Fig. 12 Tension spectrum of tethers in buoyant leg-1 under random waves

(a) PM spectrum

(b) JONSWAP spectrum

Fig. 13 Stress histogram for extreme sea state

13.02 years. The reduction in the service life is attributed to the increase in the number of stress cycles and the maximum stress range, compared to that of the normal case. The stress histogram for the extreme sea state is shown in Fig. 13.

Conclusions

The study presented the preliminary design and detailed analytical investigation of the offshore triceratops for ultra-deep waters, to illustrate the advantages of the chosen structural configuration. The salient points observed from the dynamic analysis are listed below:

1. The shift in the natural period of the structure from the wave period indicates the ease of installation under sea conditions.
2. Heave response of deck is lesser compared to the surge response. This shows that the platform is stiff in heave degree-of-freedom, which is mandatory for deep-water offshore structures.
3. The reduced pitch response in deck compared to the BLS unit shows the advantage of using the ball joints.
4. The reduced pitch response even under higher amplitude waves will also be advantageous in operating with high deck loads under harsh environmental conditions. The smaller pitch response observed in the deck is due to differential heave.

This shows that the offshore triceratops is advantageous due to the chosen structural configuration, which is found to be effective for ultra-deep waters. The preliminary design of deck and the BLS units is also carried out, to understand the suitability of the Triceratops from the member-level design perspective. As tethers are the crucial components in the complaint platforms, the stress analysis of tethers is also presented. The stress variation in the tethers is comparatively lower than the yield stress. However, fatigue analysis is also presented as tethers are subjected to periodic tension

variation. The service life of the tethers assessed from the fatigue analysis under rough sea state is approximately 20 years.

References

1. Chandrasekaran S, Jain AK (2002) Triangular configuration tension leg platform behaviour under random sea wave loads. Ocean Eng 29(15):1895–1928
2. Chandrasekaran S, Jain AK (2002) Dynamic behaviour of square and triangular offshore tension leg platforms under regular wave loads. Ocean Eng 29(3):279–313
3. Chandrasekaran S, Jain AK, Gupta A, Srivastava A (2007) Response behaviour of triangular tension leg platforms under impact loading. Ocean Eng 34(1):45–53
4. Capanoglu CC, Shaver CB, Hirayama H, Sao K (2002) Comparison of model test results and analytical motion analyses for a buoyant leg structure. In: The twelfth international offshore and polar engineering conference. International society of offshore and polar engineers
5. Copple RW, Capanoglu CC (1995)A buoyant leg structure for the development of marginal fields in deep water. In: The fifth international offshore and polar engineering conference. International society of offshore and polar engineers
6. White CN, Copple RW, Capanoglu C (2005) Triceratops: an effective platform for developing oil and gas fields in deep and ultra deep water. In: The fifteenth international offshore and polar engineering conference. International society of offshore and polar engineers
7. Chandrasekaran S, Mayanak S (2017) Dynamic analyses of stiffened triceratops under regular waves: experimental investigations. Ships Offshore Struct 12(5):697–705
8. Chandrasekaran S, Sundaravadivelu R, Pannerselvam R, Madhuri S, Varthini DS (2011) Experimental investigations of offshore triceratops under regular waves. In: Proceedings 30th international conference on ocean, offshore and arctic engineering, OMAE
9. Shaver CB, Capanoglu CC, Serrahn CS (2001) Buoyant leg structure preliminary design, constructed cost and model test results. In: The eleventh international offshore and polar engineering conference. International Society of Offshore and Polar Engineers
10. Islam AS, Soeb MR, Jumaat MZ (2017) Floating spar platform as an ultra-deepwater structure in oil and gas exploration. Ships Offshore Struct 12(7):923–936
11. Tabeshpour MR, Golafshani AA, Seif MS (2006) Comprehensive study on the results of tension leg platform responses in random sea. J Zhejiang Univ Sci A 7(8):1305–1317

12. Chen Y, Zimmer RA, de Oliveira JG, Jan HY (1985) Buckling and ultimate strength of stiffened cylinders: model experiments and strength formulations. In: Offshore Technology Conference 1985 Jan 1

13. Chandrasekaran S, Madhuri S, Jain AK (2013) Aerodynamic response of offshore triceratops. Ships Offshore Struct 8(2):123–140

14. Chandrasekaran S, Nannaware M (2014) Response analyses of offshore triceratops to seismic activities. Ships Offshore Struct 9(6):633–642

15. Chandrasekaran S, Nassery J (2015) Springing and ringing response of offshore triceratops. In: Proceedings of the 34th international conference on ocean, offshore and arctic engineering (St. John's, Newfoundland)

16. Liapis S, Bhat S, Caracostis C, Webb C, Lohr (2010). Global performance of the Perdido spar in waves, wind and current–numerical predictions and comparison with experiments. OMAE2010-2116

17. Veritas DN (2010) Buckling strength of shells, recommended practice DNV-RP-C202. Det. Nor. Ver. Class. AS, Veritasveien

18. Reddy DV, Swamidas AS (2013) Essentials of offshore structures: framed and gravity platforms. CRC Press, Boca Raton

19. Chandrasekaran S, Seeram M (2012) Stability studies on offshore triceratops. Int J Innov Res Dev 1(10):398–404

20. Chandrasekaran S, Madhuri S (2015) Dynamic response of offshore triceratops: numerical and experimental investigations. Ocean Eng 109(15):401–409

21. Jain AK, Chandrasekaran S (2004) Aerodynamic behaviour of offshore triangular tension leg platforms. In: The fourteenth international offshore and polar engineering conference. International Society of Offshore and Polar Engineers

22. DNV-RP DN (2005) C203 fatigue design of offshore steel structures. Recommended practice DNV-RPC203, p 126